FULL PAPER

Controllable Patterning of Different Cells Via Optical Assembly of 1D Periodic Cell Structures

*Hongbao Xin, Yuchao Li, and Baojun Li**

Flexible patterning of different cells into designated locations with direct cell–cell contact at single-cell patterning precision and control is of great importance, however challenging, for cell patterning. Here, an optical assembly method for patterning of different types of cells via direct cell–cell contact at single-cell patterning precision and control is demonstrated. Using *Escherichia coli* and *Chlorella* cells as examples, different cells are flexibly patterned into 1D periodic cell structures (PCSs) with controllable configurations and lengths, by periodically connecting one type of cells with another by optical force. The patterned PCSs can be flexibly moved and show good light propagation ability. The propagating light signals can be detected in real-time, providing new opportunities for the detection of transduction signals among patterned cells. This patterning method is also applicable for cells of other kinds, including mammalian/human cells.

1. Introduction

Controlling the spatial arrangement of distinct cells into well-defined patterns is of significant importance for broad biochemical and biomedicine applications such as tissue engineering,[1–3] cell-based assays,[4] drug delivery,[5] and fundamental studies of cell–cell interaction and communication.[6,7] Until now, different techniques have demonstrated the ability for cell patterning by immobilizing cells on designated regions of a surface. For example, cell patterning has been achieved by using microcontact printing[8] or lithography[9] to define the locations of cell attachment, inkjet printing[10] to place cells pixel by pixel on a substrate, dielectrophoresis[11] to use dielectrophoretic forces to concentrate cells into specific locations, and electrochemical desorption[12] to use electrochemically constrained surface changes to attach cells. In addition, by cooperating with microcontact printing, orthogonal engineering matrix can be used to regulate multicellular morphology, which suggests important ways in developing implantable materials via cell patterning.[13] Particularly, with the assistance of microfluidic systems, these techniques have shown great promise towards high throughput cell handing, culture, and analysis.[14] However, these techniques typically require elaborately fabricated substrates or electrodes to predetermine the locations of cell patterns, and they are generally used for large scale cell patterning, offering no single-cell precision and control. To investigate the proper function of a specific cell and the interaction between different patterned cells, it is highly desired to pattern different cells at designated locations precisely at single-cell patterning control. Although different methods have been used for the controllable patterning of cells into cell arrays at single-cell resolution, for example, dip-pen nanolithography[15] and optical trapping method using holographic optical tweezers,[16] they are used to pattern cells of only a single type at one time. To pattern cells of different types simultaneously at single-cell resolution, a DNA-encoding method was reported by using dense DNA microarrays for multiplexed patterning of biotinylated cells with complicated physical and biochemical procedures.[17] The patterned cells are spatially distributed with defined separations. For biomedicine applications such as drug delivery[18,19] and cell–cell interaction and communication[20] which request the cells to be directly contacted with each other, patterning cells of different types with direct contact using a simple and flexible method is highly desirable. In addition, the signal transduction among adjacent patterned cells and the response signal of the cells to the surrounding environment changes cannot be directly detected for the previously reported patterning methods. Previously, a tapered optical fiber has been used to trap cells in a controllable and flexible manner,[21,22] however, it is used for trapping of single cells of single types at one time. Here, we show that using an abruptly tapered fiber (ATF), controllable patterning of multiple cells of different types at single-cell patterning precision and control can be achieved by optical trapping. Using *Escherichia coli* (*E. coli*), which is widely used for both biological signal and drug delivery,[18–20] and *Chlorella* as living cell samples, different cells were connected with each other via direct cell–cell contact, patterning 1D periodic cell structures (PCSs) with controllable lengths and configurations, and the propagating signal along the cell structures can be detected in real-time. This method is also used for cells of other kinds, including mammalian/human cells.

H. Xin, Y. Li, Prof. B. Li
State Key Laboratory of Optoelectronic Materials and Technologies
School of Physics and Engineering
Sun Yat-Sen University
Guangzhou 510275, P.R. China
E-mail: stslbj@outlook.com

DOI: 10.1002/adfm.201500287

2. Results and Discussion

2.1. Numerical Simulation and Analysis

For cell patterning, an ATF is designed and shown in Supporting Information, Figure S1a. To get an obvious trapping

and meanwhile induce little harm to the cells, a 980 nm wavelength laser beam, which exhibits low absorption to most living matter,[23] is used. To show the possibility of cell patterning, a finite-element method was used to simulate light distribution output from the ATF. In the simulation, the *E. coli* and *Chlorella* were approximately assumed to be a nanorod (length, 1.7 μm; diameter, 0.5 μm) with hemispherical caps and a sphere (diameter, 3.2 μm), respectively. The refractive indices (n) of the ATF, water, *E. coli*, and *Chlorella* are set to be n = 1.44, 1.33, 1.39, and 1.45, respectively. The simulated light distribution is shown in Supporting Information, Figure S1b–d. Light is highly concentrated at the fiber tip because of the abruptly tapered shape, and a large optical gradient exists along the fiber axis. Compared with our previously reported gradually tapered fiber,[22] here light output from the ATF is more concentrated along the fiber axis, which allows multiple cells to be trapped by optical gradient force along the fiber axis. To show the ability of connecting multiple cells together, light distributions for cell structures with different cell number were simulated. The optical force ($\mathbf{F}_O$) exerted on the tail cell of each structure can be calculated by integrating the time-independent Maxwell stress tensor $\mathbf{T}_M$ along the surface of the cell. $\mathbf{F}_O$ can be expressed as[22]

$$\mathbf{F}_O = \oint_S (\langle \mathbf{T}_M \rangle \mathbf{n}) dS \quad (1)$$

where $\mathbf{n}$ is the surface normal vector. Calculation results show that $\mathbf{F}_O$ exerted on the *E. coli* cells are directed to the ATF, and thus the *E. coli* cells can be trapped and connected. Light is highly confined and propagated along the cells, and more cells can be trapped and connected. With a *Chlorella* cell added to the former connected *E. coli* cell, $\mathbf{F}_O$ exerted on the *Chlorella* cell is also directed to the ATF, and thus the *Chlorella* cell can be trapped and connected to the *E. coli* cells. Similarly, more cells can be trapped and connected to the former trapped cells orderly by optical force, patterning into a PCS. In Supporting Information, Figure S2 shows detailed light distributions and force calculation for cell structures with different cell numbers, showing the patterning progress of a PCS with three *E. coli* cells connecting two neighboring *Chlorella* cells. The periodic configurations of the PCSs are manually controlled. The parameters considered here are period (T, number of *E. coli* cells connecting neighboring *Chlorella* cells), neighboring *Chlorella* cell distance (D), *Chlorella* cell number (N), and structure length (L). **Figure 1**a, as examples, shows the calculated F_O exerted on the tail *Chlorella* cell of PCSs with different parameters. Calculation results show that F_O exerted on the tail *Chlorella* cell of each PCS is directed to the ATF, and thus the *Chlorella* cell can be trapped and connected to the former trapped *E. coli* cells, forming PCSs with different lengths, and light can propagate along the PCSs. Figure 1b shows light propagating along PCSs with different parameters.

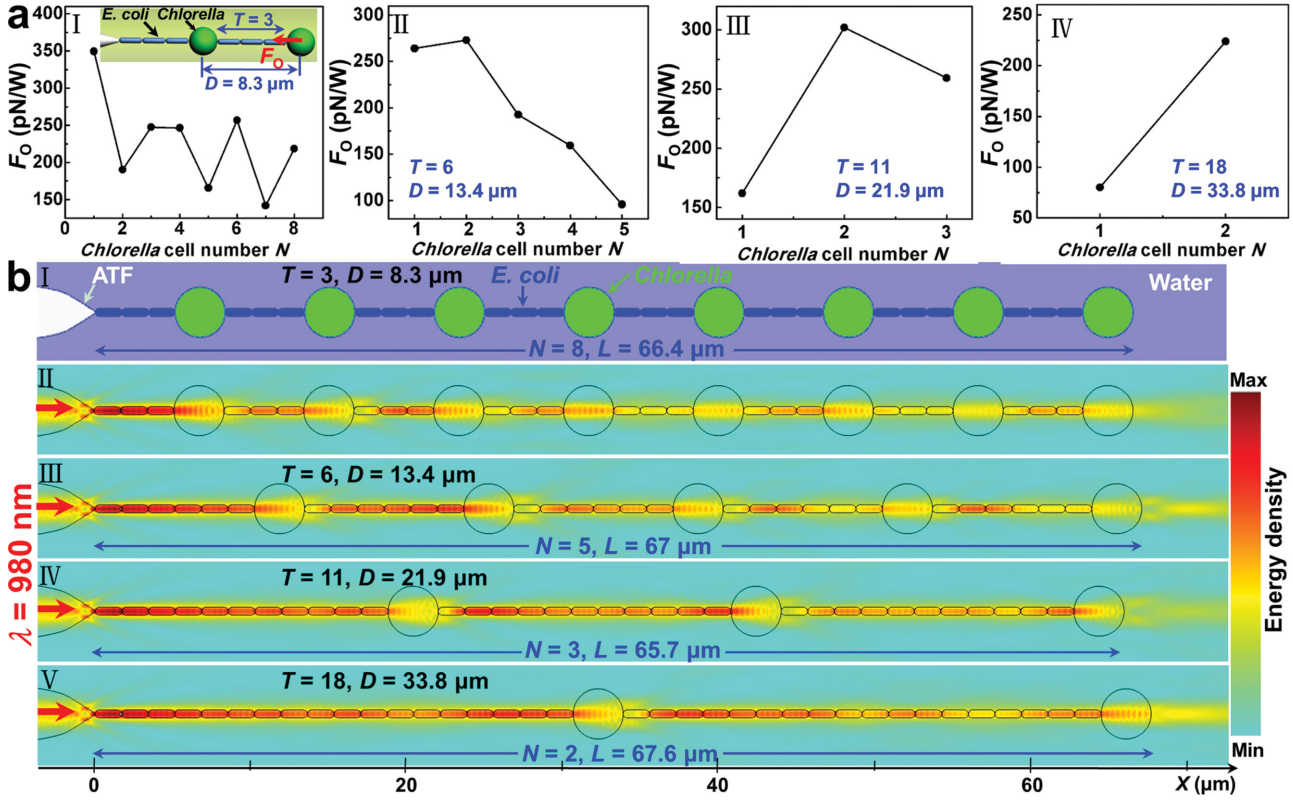

Figure 1. Simulation and calculation results for PCSs with different configurations. a) Calculated F_O exerted on the tail *Chlorella* cell as a function of *Chlorella* cell number N for PCSs with I) T = 3, D = 8.3 μm; II) T = 6, D = 13.4 μm; III) T = 11, D = 21.9 μm; and IV) T = 18, D = 33.8 μm; inset in (I) schematically shows the parameters and calculation model. b) Simulated optical energy density distributions for light propagating along the PCSs with I, II) T = 3, D = 8.3 μm, N = 8, and L = 66.4 μm; panel (I) shows the simulation model; III) T = 6, D = 13.4 μm, N = 5, and L = 67 μm; IV) T = 11, D = 21.9 μm, N = 3, and L = 65.7 μm; and V) T = 18, D = 33.8 μm, N = 2, and L = 67.6 μm.

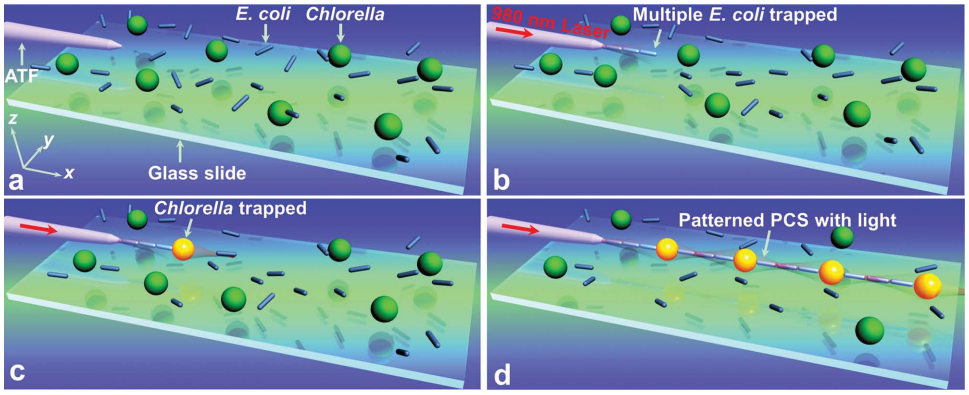

Figure 2. Experimental schemes for cell patterning. a) An ATF is placed in cell suspensions. b) Laser launched, multiple *E. coli* cells trapped. c) A *Chlorella* cell is trapped and connected to the former trapped *E. coli* cells. d) A PCS is formed, and light propagates along the PCS.

2.2. Experimental Results

Based on the above analysis, an experimental scheme is designed in **Figure 2**. An ATF is immersed in a mixture suspension of *E. coli* and *Chlorella* cells (Figure 2a) (see Experimental Section for suspension preparation). With a laser beam (980 nm wavelength) launched into the ATF, by moving the ATF, multiple *E. coli* near the ATF tip can be trapped orderly by optical trapping (Figure 2b). By moving the ATF toward a *Chlorella*, the *Chlorella* can be trapped and connected to the former trapped *E. coli* (Figure 2c) by F_O. By moving the ATF and/or the glass slide, more cells will appear near the former trapped cells. These cells can then be trapped and connected to the former trapped cells, forming PCSs with different configurations at single-cell control, and light can propagate along the PCSs (Figure 2d). The moving of the ATF and the glass slide is controlled by a six-axis fiber positioner, which can be flexibly moved in 3D and a 2D translation stage, respectively, both with 50 nm precision. Light propagating along the PCSs can be detected using a tapered optical fiber (TF) directly contacting the end of the PCSs, and the signal is collected and analyzed by an optical power meter in real-time. Details of the experimental setup are shown in Supporting Information, Figure S3 with a scanning electron microscope (SEM) image of the ATF used in the experiments. The ATF is of high fabrication reproducibility (see Experimental Section for ATF fabrication) and can result in a stable trapping.

Figure 3a shows a typical SEM image of the *E. coli* cells, while Figure 3b,c shows the length and diameter distributions of the *E. coli* cells statistically analyzed on a population of more than 100 cells. The average values of the *E. coli* diameter and length are 0.5 and 1.7 μm, respectively. Figure 3d,e shows the optical microscope image of the *Chlorella* cells and the mixture of *E. coli* and *Chlorella* cells, respectively. The diameter distribution of the *Chlorella* cells is shown in Figure 3f by statistically analyzing on a population of more than 100 cells, with an average value of 3.2 μm. To show the potential for light propagation along the PCSs formed by the cells, a typical ultraviolet–visible–near infrared (UV–vis–NIR) absorption spectrum analysis was carried out as shown in Figure 3g. Results show that both the cells of single type and the mixture show a low absorption in the visible and near infrared spectrum, indicating a suitability of light in the visible and near infrared regions to propagate along the PCSs formed by these cells with small photo-damage. It should be noted that a clear kink for the absorption spectrum of the *Chlorella* cells and the cell mixture exists in the wavelength range of about 670–890 nm, this is because the chlorophyll inside the *Chlorella* cells exhibit a higher absorption of light in this wavelength range.

To start experiments, the laser beam with an optical power of 57 mW (measured at the output of the laser source) was launched into the ATF immersed in the suspensions. With the laser beam launched, *E. coli* and *Chlorella* cells near the ATF tip were trapped by F_O, forming PCSs with different configurations, and the locations of the *Chlorella* cells were manually controlled. **Figure 4**aI–VI, as examples, show the assembled PCSs with (D = 11.5 μm, L = 40.9 μm), (D = 17.2 μm, L = 63.1 μm), (D = 22.2 μm, L = 81.8 μm), (D = 30.4 μm, L = 98.8 μm), (D = 35.1 μm, L = 71.3 μm), and (D = 42.1 μm, L = 86.5 μm), respectively. It should be noted that resulting from the uneven size distributions of the cells, a maximum deviation of about ±2.0 μm exists for the D values in the same PCSs. The Supporting Information, Figure S4, as an example, shows the detailed patterning process of a PCS with an average D = 11.5 μm and L = 42.1 μm at single-cell patterning control. Remarkably, besides PCSs with *E. coli* connecting single *Chlorella* cells, PCSs with *E. coli* connecting *Chlorella* cell groups can also be patterned. Figure 4b shows a patterned PCS with *E. coli* connecting *Chlorella* cell groups (two *Chlorella* cells in each group), with an average distance between the neighboring *Chlorella* cell groups of 15.8 μm and L = 58.1 μm. Besides the patterning of PCSs, cell structures with other configurations can also be patterned. Figure 4c, as an example, shows a patterned 1D cell structures with arithmetic progression configuration and L = 86.5 μm. The distances from the first *Chlorella* cell to the ATF tip and that between the neighboring *Chlorella* cells are 35.7, 26.9, and 18.1 μm, respectively. It should be noted that for a PCS with L > 100 μm, the distance between the tail *Chlorella* cells is difficult to keep stable when moving the ATF and/or the glass slide. However, cell structures with L > 100 μm can also be formed. Figure 4d, as an example, shows a patterned structure with L = 130 μm, and the distances between neighboring *Chlorella* cells are 23.9, 22.2, 33.9, 18.7, and 9.4 μm from left to right. Experimental results also show that the cellular shape makes little effect on the patterning. For

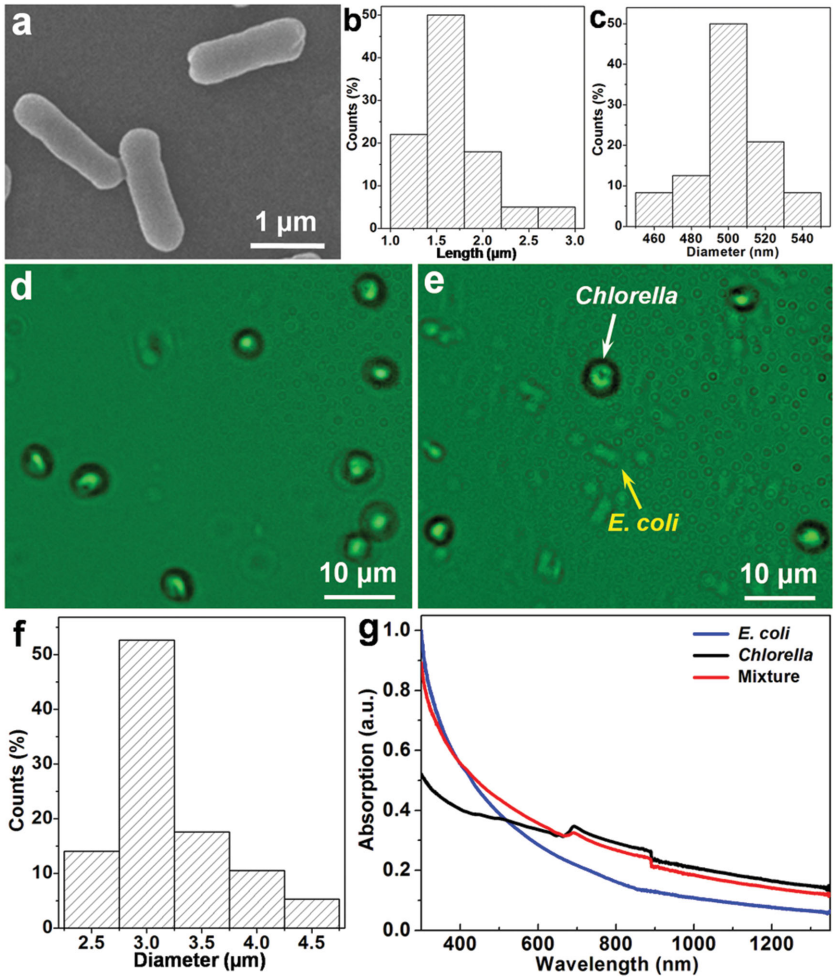

Figure 3. Characterization of the cells. a) SEM images of the *E. coli* cells. b) Length distribution of the *E. coli* cells. c) Diameter distribution of the *E. coli* cells. d,e) Optical microscope images of d) the *Chlorella* cells and e) mixture of the *E. coli* and *Chlorella* cells. f) Diameter distribution of the *Chlorella* cells. g) Optical absorption spectrum of the *E. coli*, *Chlorella*, and mixture of *E. coli* and *Chlorella* cells.

example, we find that *E. coli* cells with different lengths and *Chlorella* cells with elliptical and other irregular shapes can also be used for the PCSs formation. Further experiments show that the stability of the formed PCSs is depended on the trapping laser. Once the laser is turned off, the formed PCSs are gradually disassembled because of Brownian motion and *E. coli* motility.

The formed PCSs can be manipulated in 3D and flexibly moved to designated locations. **Figure 5**a,b shows the moving of PCSs with *E. coli* cells connecting single *Chlorella* cells (average *D*, 12.3 μm; *L*, 43.3 μm) and *Chlorella* cell groups (average *D*, 16.3 μm; *L*, 54.4 μm) in *x* direction, respectively. The PCSs were moved with respective distances of 39.8 and 76.8 μm both within 3 s. The moving velocity and distance of the PCSs are controlled by moving the fiber positioner.

To show the effect of light on the cell physiology after patterning, additional experiments on cell viability have been carried out. Because light intensity was decreased along the PCSs, thus cells close to the ATF tip may be influenced most by the trapping laser due to the stronger light intensity. We have thus paid particular attention on the cells trapped near the ATF tip. As an example, Supporting Information, Figure S5 shows the growth and division of *E. coli* cells in the trapping, indicating that the survivability of the *E. coli* cells was not affected by the trapping laser. For the *Chlorella* cells, because the complete division cycle is about 20 h, direct observation of the division was not observed during the trapping. However, because during the patterning, the *Chlorella* cells were trapped after the *E. coli*, and light intensity on the *Chlorella* cells was smaller than that on the *E. coli* cells, thus photo damage on the *Chlorella* cells was even much smaller than that on the *E. coli* cells. Thus, light makes no direct damage on the cell physiology of the cells after patterning. This is because the optical power of the laser is relatively low (about 50–70 mW), and the 980 nm wavelength laser beam is weakly absorbed by the cells.[23]

Because the cell structures are formed by optical force, this indicates that light can propagate along the formed PCSs. To detect the propagating optical signal in real-time, a TF connecting to an optical power meter was connected to the tail cell of the PCS. The real-time propagating signal can then be observed. Using the method schematically shown in the inset of Figure 4e, the propagation loss (α) for light along the PCSs can be measured. First, the TF was connected to the PCS with a length of L_1 formed with an optical power of P_0. The propagating light along the PCS was collected by the TF, and the measured output optical power is P_1. With the same input P_0, when the length of the PCS was increased to L_2, an output power of P_2 was then measured. The measured propagation loss can be obtained by[24]

$$\alpha = \frac{10}{L_2 - L_1} \log\left(\frac{P_1}{P_2}\right) \quad (2)$$

The measured α for the propagating 980 nm light along different PCSs with different *D* is shown in Figure 4e. It can be seen that α is decreased with the increasing *D*. This is because PCS with a smaller neighboring *Chlorella* cell distance can result in a larger scattering loss by the denser *Chlorella* cells when directly connected to the *E. coli* cells due to the different sizes and optical properties.

To show light propagating along the PCSs, a 644 nm red laser beam was launched into the PCSs while remain the optical power of 980 nm laser beam for the PCSs formation unchanged (see Supporting Information, Figure S3a for the coupling of the two laser beams). **Figure 6** shows the PCSs with both 980 nm and 644 nm laser beams launched. The optical

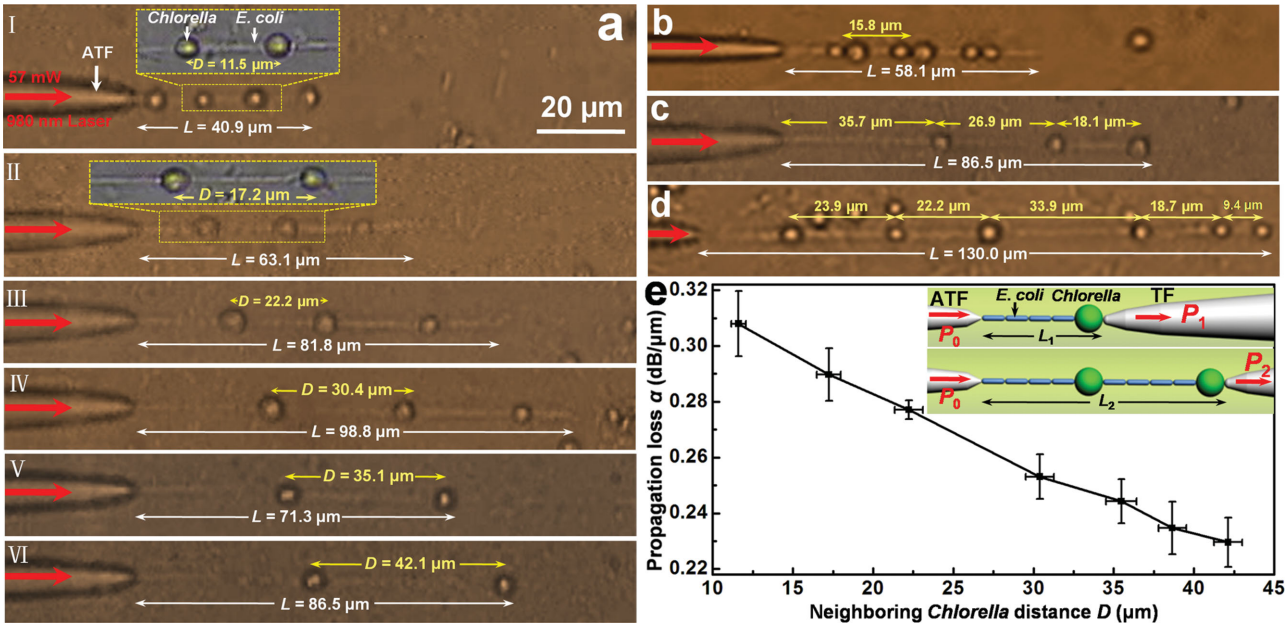

Figure 4. Optical microscope images and propagation loss of PCSs with different configurations. a) Images for PCSs with different *D* and *L*. Red arrows indicate the input laser (57 mW), insets in (I) and (II) are the enlarged images of the PCSs showing the *Chlorella* and *E. coli* cells contact. b) Image for a 1D structure with *E. coli* cells connecting *Chlorella* cell groups. c) Image for a structure exhibiting arithmetic progression characteristic for *Chlorella* cell distances. d) Image for a structure with $L = 130.0$ μm. e) Propagation loss α of PCSs as a function of neighboring *Chlorella* cell distance *D*, inset shows the loss calculation schematic.

power of the 980 nm laser beam for all the PCSs formation was 65 mW. For PCSs with different lengths of 58.8, 60.2, 65.1, 80.2, and 82.5 μm and *Chlorella* cell numbers of 2, 3, 4, 5, and 7 as, respectively, shown in Figure 6a–e, due to the propagation loss, to observe the propagating of 644 nm red light, the optical power of the 644 nm laser beam was set to be 25, 25, 28, 30, and 33 μW, respectively. It can be seen that resulting from the scattering of the *Chlorella* cells, red spots were observed periodically. Particularly, red spots appeared at the PCSs output. These red spots intuitionally indicate that 644 nm red light propagates along the PCSs. This confirms that light can propagate along the PCSs.

2.3. Discussion

Both the above simulation and experimental results show that cells with different types can be controllably patterned via optical assembly of 1D PCSs with different lengths and configurations, and light can be propagated along the PCSs. However, it is highly desirable to pattern cells with different sizes for various medical applications, particularly, for mammalian/human cells with sizes of about 10–30 μm. To show the possibility of patterning cells with different sizes, simulation on cells with 3 levels of sizes have been carried out. In the simulation, *E. coli* cells (rod-shaped bacteria, 1.7 μm in length and

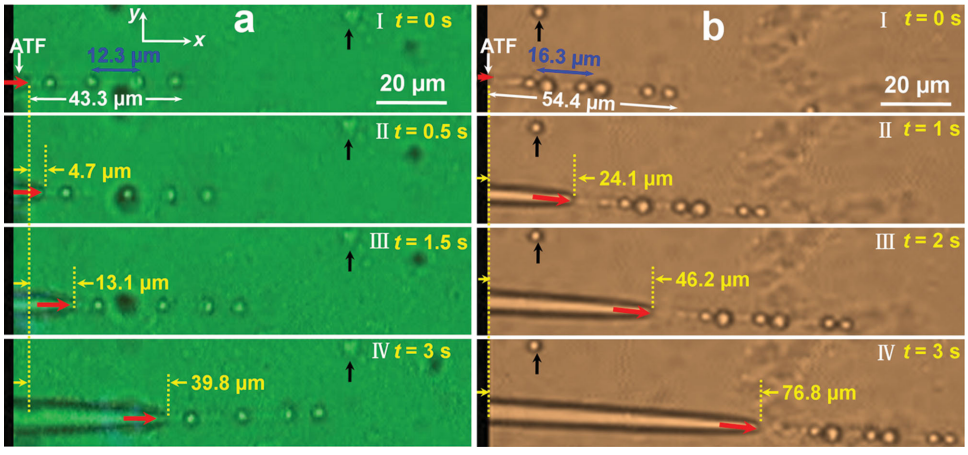

Figure 5. Optical microscope images for PCSs moving. The red arrows indicate the input laser (57 mW). a) Moving of a PCS with *E. coli* cells connecting single *Chlorella* cells. The yellow dashed lines and black arrows indicate the input end of the PCS and the reference objects sticking on the glass slide in the moving process, respectively. b) Moving of a PCS with *E. coli* cells connecting *Chlorella* cell groups.

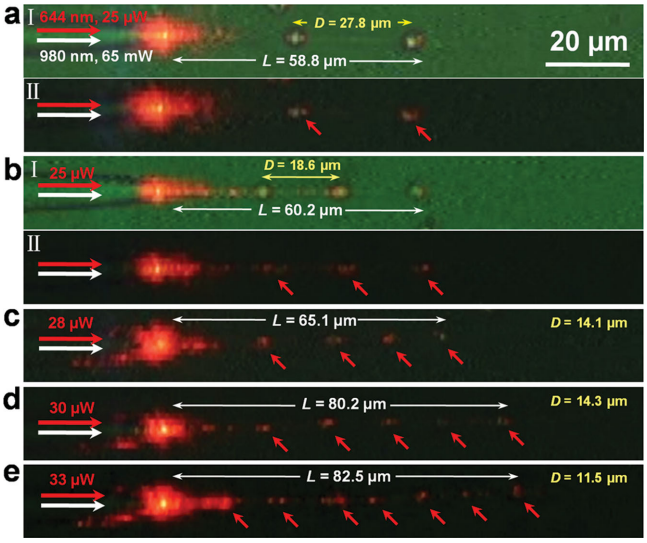

Figure 6. Optical microscope images for light propagation along PCSs. The horizontal white and red arrows indicate the 980 nm (65 mW) and 644 nm wavelength laser beams, respectively, while the slanted red arrows indicate the red light spots. a) For PCS with $L = 58.8$ μm and average $D = 27.8$ μm, panels I and II show the bright field and dark field images, respectively. b) PCS with $L = 60.2$ μm and average $D = 18.6$ μm. c) PCS with $L = 65.1$ μm and average $D = 14.1$ μm. d) PCS with $L = 80.2$ μm and average $D = 14.3$ μm. b) PCS with $L = 82.5$ μm and average $D = 11.5$ μm.

0.5 μm in diameter, $n = 1.39$), yeast cells (spherical eukaryotes, 4.5 μm in diameter, $n = 1.40$), and human leukemia K562 cells (spherical human cells, 15 μm in diameter, $n = 1.41$) are used as the examples of 1 μm (small bacteria), 2–5 μm (larger bacteria and small eukaryotes), and 10–30 μm (mammalian cells) cells, respectively. Simulation results show that all of these three kinds of cells can be trapped by the ATF, and light can be propagated along the trapped and patterned cell structures. As an example, **Figure 7**aI–III shows light propagating along the patterned *E. coli* (cell number $N = 20$), yeast ($N = 10$), and K562 ($N = 10$) cell structures, respectively. By calculating the optical force (F_O) exerted on the tail cell of each structure with different cell numbers, results show that F_O is directed to the ATF (trapping force) and cells with different sizes can be trapped by the exerted optical trapping force. Multiple cells can then be assembled along the ATF, patterning into 1D cell structures. Figure 7b–d shows the calculated F_O exerted on the tail cell of cell structures with different cell numbers for *E. coli*, yeast, and K532 cells, respectively.

To experimentally show the ability of patterning cells with different sizes, similar to the above simulation, *E. coli* (average length: 1.7 μm, average diameter: 0.5 μm), yeast (average diameter: 4.5 μm), and human leukemia K562 (average diameter: 15 μm) cells, are used as cell samples. Experimental results show that all these three kinds of cells can be trapped and patterned into 1D cell structures using the method shown in Figure 2. **Figure 8**, as some examples, shows the patterned cell structures with different cells. With the 980 nm laser (optical power: $P = 17$ mW) launched into the ATF, an *E. coli* cell structure with cell number of $N = 7$ and length of $L = 13.4$ μm was formed (Figure 8aI). By increasing the optical power to 32 mW, an *E. coli* cell structure with ($N = 17$, $L = 33.1$ μm) was formed (Figure 8aII). For the yeast cells, with $P = 25$ and 45 mW launched into the ATF, cell structures with ($N = 4$, $L = 17.5$ μm) and ($N = 8$, $L = 38.7$ μm) were formed, as respectively shown in Figure 8bI,II. Similarly, for the K562 cells, with $P = 45$ and 80 mW launched into the ATF, cell structures with ($N = 4$, $L = 66.1$ μm) and ($N = 8$, $L = 121.3$ μm) were formed, as respectively shown in Figure 8cI,II. These results show that this patterning method is applicable for cells with different sizes. By simply mixing different cells together, PCSs with different configurations can be formed by using the method shown in Figure 2.

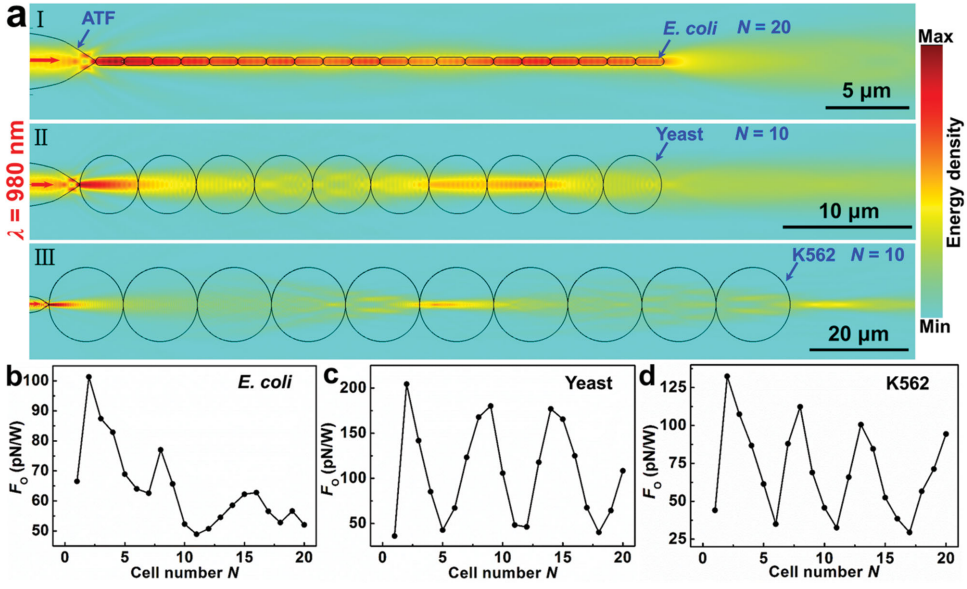

Figure 7. Simulation and calculation results for cell structures patterned with different cells. a) Simulated optical energy density distributions for cell structures patterned with I) *E. coli* cells (cell number $N = 20$), II) yeast cells ($N = 10$), and III) K562 cells ($N = 10$). b–d) Calculated optical trapping force (F_O) exerted on the tail cell of the structures with cell number N for b) *E. coli* cells, c) yeast cells, and d) K562 cells.

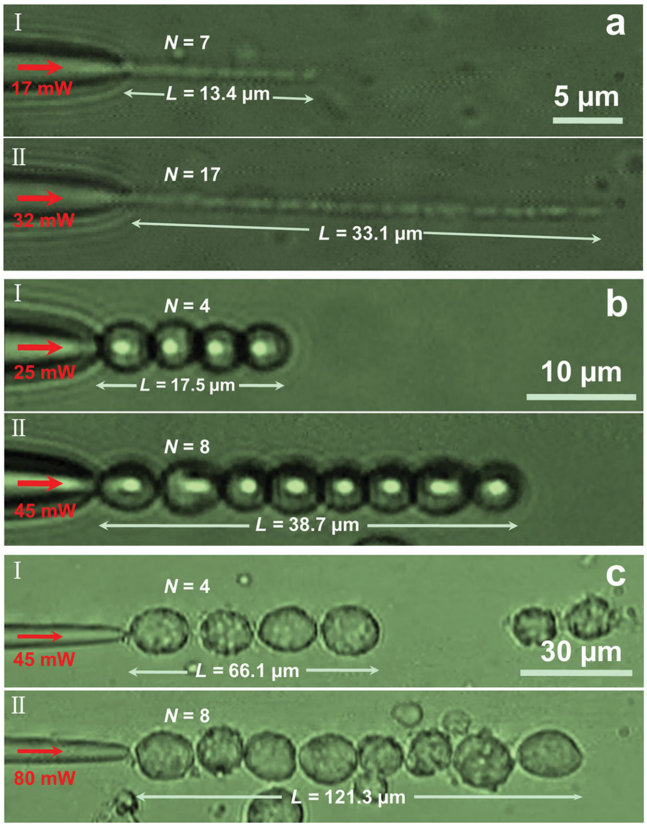

Figure 8. Optical microscope images for 1D cell structures formed with different cells. The red arrows indicate the input 980 nm laser. a) For *E. coli* cells. b) For yeast cells. c) For K562 cells.

Although cells with different sizes can be patterned, the patterning ability is different. From the force calculation results for cells with three levels of sizes (Figure 7b–d), it can be seen that the maximum trapping force for the 4.5 μm yeast cells is the largest, while that for the *E. coli* cells is the smallest. However, resulting from the quasi-periodically focusing and diverging of light along the large spherical yeast and K562 cells along the cell structures, force is also quasi-periodically changed, with peak values and valley values quasi-periodically appeared. These valley values of force increase the difficulty for cell patterning. In addition, from the experiments we find that for cells with a larger size, they sink easier and stick to the glass slide easier, resulting from the increasing weight. This further increases the difficulty for PCS design with larger cells. Therefore, the increasing in cell sizes increases the difficulty for PCSs design. To pattern and design PCSs for cells with larger sizes, a larger input optical power should be launched into the ATF as shown in Figure 8. However, the increasing optical power may increase the photodamage to the cells. Thus the potential limitation and disadvantage of the system is the photodamage to the cells by the laser beam for PCSs design with larger cells. Fortunately, this photodamage can be minimized by choosing a laser beam at a wavelength with low absorption to the cells or decreasing the laser radiation duration.

Compared with the previously reported cell patterning methods, such as microcontact printing,[8] lithography,[9] inkjet printing,[10] dielectrophoresis,[11] and electrochemical desorption,[12] the main advantages of our method are 1) the method is very simple with only a single ATF and a laser source, without the need of elaborately fabricated substrates of electrodes to predetermine the locations of cell patterns; 2) the patterning offers single-cell precision and control; 3) cells of different types can be controllable positioned into designated locations, forming cell structures with periodic configurations via direct cell–cell contact; 4) the patterned cell structures can be flexibly moved in 3D to designated locations; 5) the optical signal propagating along the cell structures can be detected in real-time. Compared with the optical trapping method using optical tweezers for cell patterning by trapping multiple cells,[16] the main advantages of this method are setup simplicity and manipulation flexibility. For cell patterning with optical tweezers, the setup structure is relatively bulky with a high-numerical-aperture focusing objective and a series of lens for beam steering and amplitude modulation,[22] and additional complicated devices such as acoustooptic deflectors and spatial light modulator are necessary for multiple cell trapping;[16] while for our method, a single tapered optical fiber can realize light delivery, focusing, and multiple cell trapping, which is much more simple and handy. To spatially move and manipulate the trapped cells, one should control the focus by beam steering and amplitude modulation elements incorporated in the optical path before the laser beam enters the focusing objective using optical tweezers; while for our method, the moving and manipulating of the trapped cells can flexibly controlled by adjusting the fiber positioner. Because the configurations of the patterned cells are manually controlled at single-cell precision, thus proper functions of cell structures can be controlled by precisely positioning different cell types in designated locations. Because the propagating signal along the PCSs can be directly detected and analyzed in real-time, this cell patterning method opens up possibilities in photonic sensing as well as detection of biological signal and transduction information among the patterned cells, particularly the response signal of the cells to the surrounding environment changes. Because the *E. coli* bacteria are directly contacted with the *Chlorella* cells in the PCSs, this strategy provides potential use for study of biological phenomena via direct cell–cell contact between different cells. For example, if the *Chlorella* cells are replaced by target cells, and the *E. coli* bacteria are loaded with drug, the PCSs patterned with these cells can be used for therapeutic applications[18,19] by delivery the drug from the *E. coli* bacteria to the target cells in a controlled route. However, additional steps may be needed when using this cell–cell contact method for drug delivery study. For example, a second laser source may be used to observe the fluorescent labeled drug delivered from the bacteria to the target cells. Note that, during the drug delivery process, the bacteria loaded with drug may be devoured by the target cells in order to deliver the drug carried by the bacteria,[19] and the optical pathway constructed by the cell–cell contact seems to be destroyed. Fortunately, the bacteria beside the patterned structures can be trapped to the PCS by transverse optical gradient force and take the place of the previously devoured bacteria, thus the optical pathway can be reconstructed and drug delivery can be continued. In addition, if the *Chlorella* cells are replaced by the host cells of the bacteria, the PCSs patterned with these cells would provide a new approach for the study of secretion signals

delivery and cell–cell communication between the bacteria and the host cells.[20] Note that although the cells are patterned into 1D structures, this strategy could be easily expanded for 2D and even 3D cell patterning by using multiple ATFs.

3. Conclusions

In summary, an optical assembly strategy for controllable patterning of different cells via direct cell–cell contact at single-cell control was demonstrated. With a 980 nm laser beam launched into an ATF, 1D PCSs with different configurations and lengths were assembled by direct connecting *E. coli* and *Chlorella* cells. The patterned cell structures can be flexibly moved, and the propagation signal along PCSs can be detected in real-time. This cell patterning method is applicable for cells of different kinds, including mammalian/human cells. This strategy provides a new approach for cell patterning with controllable cell locations at single-cell control, and provides possibilities for biological discoveries via direct cell–cell contact between different living cells and real-time signal sensing and detection.

4. Experimental Section

Methods for Fabrication of ATF: A commercial single-mode optical fiber (connector type: FC/PC; core diameter: 9 μm; cladding diameter: 125 μm; Corning Inc.) was used for fabricating the ATF using a flame-heating method.[22] Before heating, a glass capillary (length: ≈120 mm; inner diameter: ≈0.9 mm; wall thickness: ≈0.1 mm) was used to sheathe the fiber whose buffer and polymer jacket were stripped off using a fiber stripper. The fiber was then kept heating for about 100 s until reaching the melting point. By applying a pulling speed of about 3 mm s^{-1} on the heating region, the fibre was broken with an abrupt tapered tip, and an ATF was fabricated.

Methods for Cell Suspensions Preparation: The *E. coli* bacteria (DH5α) were grown overnight at 37 °C in Luria-Bertani medium, washed in phosphate buffered saline (PBS) buffer and resuspended in the PBS buffer (diluted with deionized water) to desired concentration (*E. coli* cell density ≈ 3.0×10^6 cells per mL). The *Chlorella* cells suspension was purchased from a biological cells supplier, and then diluted with deionized water to desired concentration (Chlorella cell density ≈ 3.0×10^5 cells per mL). The mixture suspension of the *E. coli* bacteria and Chlorella cells was prepared by mixing the prepared *E. coli* suspension and *Chlorella* suspension together (volume ratio of the *E. coli* suspension to *Chlorella* suspension ≈ 1:2). To ensure the cell mixture in dispersed state, the suspension was kept in a static state for ≈10 min. After preparation, the mixture suspension was dripped onto the surface of a glass slide using a pipette for ATF immersion. The yeast cells suspension was purchased from a biological cells supplier, and diluted with deionized water to desired concentration (cell density ≈ 3.0×10^5 cells per mL). The human leukemia K562 cells were directly purchased from Laboratory Animal Center of Sun Yat-Sen University, and diluted with PBS to desired concentration (cell density ≈ 2.0×10^5 cells per mL).

Supporting Information

Supporting Information is available from the Wiley Online Library or from the author.

Acknowledgements

The authors greatly thank Ms. Haifang Wang from School of Pharmaceutical Sciences, Sun Yat-Sen University for the preparation of *E. coli* bacteria and Mr. Xiaodong Chen from School of Physics and Engineering, Sun Yat-Sen University for the fruitful assistance in the simulation. This work was supported by the National Natural Science Foundation of China (Grant Nos. 11274395 and 61205165), the Program for Changjiang Scholars and Innovative Research Team in University (IRT13042). The citation of the ATF fabrication method in the Experimental Section was corrected on May 18, 2015.

Received: January 23, 2015
Revised: March 2, 2015
Published online: March 30, 2015

[1] A. Khademhosseini, R. Langer, J. Borenstein, J. P. Vacanti, *Proc. Natl. Acad. Sci. USA* **2006**, *103*, 2480.
[2] N. W. Choi, M. Cabodi, B. Held, J. P. Gleghorn, L. J. Bonassar, A. D. Stroock, *Nat. Mater.* **2007**, *6*, 908.
[3] B. Derby, *Science* **2012**, *338*, 921.
[4] K. Ino, M. Okochi, N. Konishi, M. Nakatochi, R. Imai, M. Shikida, A. Ito, H. Honda, *Lab Chip* **2008**, *8*, 134.
[5] W. M. Saltzman, W. L. Olbricht, *Nat. Rev. Drug Discov.* **2002**, *1*, 177.
[6] Z. Chen, Y. Li, W. Liu, D. Zhang, Y. Zhao, B. Yuan, X. Jiang, *Angew. Chem. Int. Ed.* **2009**, *48*, 8303.
[7] B. Yuan, Y. Li, D. Wang, Y. Xie, Y. Liu, L. Cui, F. Tu, H. Li, H. Ji, W. Zhang, X. Jiang, *Adv. Funct. Mater.* **2010**, *20*, 3715.
[8] S. A. Ruiz, C. S. Chen, *Soft Matter* **2007**, *3*, 168.
[9] I. S. Carrico, S. A. Maskarinec, S. C. Heilshorn, M. L. Mock, J. C. Liu, P. J. Nowatzki, C. Franck, G. Ravichandran, D. A. Tirrell, *J. Am. Chem. Soc.* **2007**, *129*, 4874.
[10] M. Singh, H. M. Haverinen, P. Dhagat, G. E. Jabbour, *Adv. Mater.* **2010**, *22*, 673.
[11] J. Ramón-Azcón, S. Ahadian, R. Obregón, G. Camci-Unal, S. Ostrovidov, V. Hosseini, H. Kaji, K. Ino, H. Shiku, A. Khademhosseini, T. Matsue, *Lab Chip* **2012**, *12*, 2959.
[12] Y. Li, B. Yuan, H. Ji, D. Han, S. Chen, F. Tian, X. Jiang, *Angew. Chem. Int. Ed.* **2007**, *46*, 1094.
[13] B. Hu, W. Shi, Y. L. Wu, W. R. Leow, P. Cai, S. Li, X. Chen, *Adv. Mater.* **2014**, *26*, 5786.
[14] S. M. Kim, S. H. Lee, K. Y. Suh, *Lab Chip* **2008**, *8*, 1015.
[15] J. Kim, Y.-H. Shin, S.-H. Yun, D.-S. Choi, J.-H. Nam, S. R. Kim, S.-K. Moon, B. H. Chung, J.-H. Lee, J.-H. Kim, K.-Y. Kim, K.-M. Kim, J.-H. Lim, *J. Am. Chem. Soc.* **2012**, *134*, 16500.
[16] G. M. Akselrod, W. Timp, U. Mirsaidov, Q. Zhao, C. Li, R. Limp, K. Timp, P. Matsudaira, G. Timp, *Biophys. J.* **2006**, *91*, 3465.
[17] U. Vermesh, O. Vermesh, J. Wang, G. A. Kwong, C. Ma, K. Hwang, J. R. Heath, *Angew. Chem. Int. Ed.* **2011**, *50*, 7378.
[18] D. Akin, J. Sturgis, K. Ragheb, D. Sherman, K. Burkholder, J. P. Robinson, A. K. Bhunia, S. Mohammed, R. Bashir, *Nat. Nanotech.* **2007**, *2*, 441.
[19] C. Zhu, Q. Yang, F. Lv, L. Liu, S. Wang, *Adv. Mater.* **2013**, *25*, 1203.
[20] J. E. Galịn, H. Wolf-Watz, *Nature* **2006**, *444*, 567.
[21] S. K. Mohanty, K. S. Mohanty, M. W. Berns, *J. Biomed. Opt.* **2008**, *13*, 054049.
[22] H. Xin, R. Xu, B. Li, *Sci. Rep.* **2012**, *2*, 818.
[23] F. M. Fazal, S. M. Block, *Nat. Photon.* **2011**, *5*, 318.
[24] J. Bigeon, N. Huby, J.-L. Duvail, B. Bêche, *Nanoscale* **2014**, *6*, 5309.